Evidence-theory-based analysis for structural-acoustic field with epistemic uncertainties

†Jian Liu[1], *Longxiang Xie[2], Xianfeng Man[3], and Yongchang Guo[4]

[1]State Key Laboratory of Advanced Design and Manufacturing for Vehicle Body, Hunan University, Changsha, Hunan 410082, China.

[2]State Key Laboratory of Advanced Design and Manufacturing for Vehicle Body, Hunan University, Changsha, Hunan 410082, China.

[3]State Key Laboratory of Advanced Design and Manufacturing for Vehicle Body, Hunan University, Changsha, Hunan 410082, China.

[4]State Key Laboratory of Advanced Design and Manufacturing for Vehicle Body, Hunan University, Changsha, Hunan 410082, China.

*Presenting author: d_x20140920@126.com

†Corresponding author: JianL2004@126.com

Abstract

Evidence theory has a strong capacity to deal with epistemic uncertainty, in view of the overestimation in interval analysis, the responses of structural-acoustic problem with epistemic uncertainty could be untreated. In this paper, a numerical method is proposed for structural-acoustic system response analysis under epistemic uncertainties based on evidence theory. To improve the calculation accuracy and reduce the computational cost, the interval analysis technique and radial point interpolation method are adopted to obtain the approximate frequency response characteristics for each focal element, and the corresponding formulations of structural-acoustic system for interval response analysis are deduced. Numerical examples are introduced to illustrate the efficiency of the proposed method.

Key words: Structural-acoustic system response analysis; Evidence theory; Radial point interpolation method; Interval analysis; Finite element method; Epistemic uncertainty

Introduction

In the last two decades, with the increasing of people's interest in the performance of NVH (noise, vibration and harshness), researches on the structural-acoustic field have been experienced a rapid development in engineering [1-3]. In most engineering cases, the structural-acoustic problems have been analysed by Probabilistic methods, in which the probability distribution, the boundary conditions and the external loads are defined unambiguously. However, due to the effects of manufacturing/assembling errors, original algorithm defect, imprecise environment factors and external excitations, uncertainties associated with geometric tolerances, material properties

and boundary conditions are unavoidable [4,5]. Generally, uncertainty can be divided into epistemic and aleatory categories based on the source of uncertainty. Epistemic uncertainty is related to the incomplete knowledge or imprecise information in any activity, which can be reduced by collecting more knowledge or experimental data. Aleatory uncertainty, on the other hand, derives from inherent variation in a physical system or environment, which is always regarded as random variables in probability theory [6]. Numerous mathematical theories or methods are developed to deal with the structural-acoustic problems under epistemic uncertainties, including possibility theory, D-S evidence theory, Bayesian theory, interval analysis, p-box method, Monte–Carlo method, spectral stochastic method, etc [7-9].

Among the approaches above, evidence theory seems to be more capable or more flexible to define epistemic uncertainty in the practical engineering problems. According to the D-S theory, it defines BPAs (basic probability assignment) to each focal element, which can provide corresponding formulations as possibility theory. Besides, the basic axioms in evidence theory can also deal with hybrid uncertainties in which aleatory and epistemic uncertainties combined in a very natural way. Thus, evidence theory has been widely used in artificial intelligence related fields and has been extended to conduct engineering structures and mechanical systems design, and reliability analysis, recently. The benefits and drawbacks of evidence theory in reliability analysis were summed by Oberkampf and Helton through a simple algebraic function [10]. An evidence-theory-based reliability analysis method was developed by Jiang et al., in which the concept of focal element was proposed firstly [11,12]. H. R. Bae proposed an efficient method based on evidence theory for reliability analysis using a multi-point approximation [13,14]. Helton et al. combined evidence theory with sampling-based sensitivity analysis when determining the epistemic uncertainty in model inputs [15]. A non-probability convex model was created by Elishakoff et al. to handle uncertain problems without sufficient information [16]. Qiu et al. proposed an interval perturbation method for narrow parameter intervals due to the unpredictable effect of neglecting the higher order terms of Taylor series or Neumann series [17]. An exploration of evidence theory has been conducted by J. C. Helton by using three uncertain quantification methods to address the challenge problems at model predictions [18]. An evidence-theory-based interval method was proposed by Rao et al. to analyse uncertain structural systems [19]. The application of fuzzy set theory in finite element method had developed the fuzzy finite element method (FFEM) for non-deterministic models [20–23]. Bae et al. applied an efficient method under a multi-point approximation to process evidence-theory-based reliability analysis [24,25]. The evidence theory and Bayesian theory were used for decision-making problems to compare the effectiveness of uncertainty quantification [26].

The response characteristics of structural-acoustic system is one of the hot points in noise prediction, which is important for NVH performance in engineering design and manufacturing [27]. From the works above, some inspiring progresses have been made for the response analysis of structure-acoustic coupling system with epistemic

uncertainties and evidence-theory-based reliability analysis. However, from an overall perspective, research on the hybrid uncertain analysis and response characteristics of complex system are still at the very beginning. Moreover, some crucial issues have not yet been solved [28]. Traditional numerical methods for the structural–acoustic problems are possibility theory or FEM (Finite Element method) in which the parameters are always regarded as random variables and the probability distributions are defined unambiguously. This assumption would ignore the influence of uncertainty and correlation in complex system [29].

In this paper, an evidence-theory-based radial point interpolation method (DSRPIM) is proposed for structure-acoustic coupling system under epistemic uncertainties, which can acquire the frequency response characteristics of complex system. The remainder of this paper is organized as follows. In chapter 2, the fundamentals of evidence theory are introduced. The equilibrium equation for structure-acoustic coupling system is deduced in chapter 3. In chapter 4, DS-RPIM is proposed to predict the frequency response characteristics of structural-acoustic problems. Two numerical examples are investigated in chapter 5. In chapter 6, some conclusions are given.

1. Evidence theory

1.1. Fundamentals of evidence theory

Evidence theory, also called as DS (Dempster-Shafer) theory, was firstly introduced by Dempster through studying statistical problems in 1976. And further developed by Shafer who defined probability to make it more suitable for general cases [30]. Compared with probability theory, evidence theory uses a prior probability distribution to get a posterior evidence interval, which quantifies the belief and plausibility of each proposition to handle the uncertainty in system response.

As probability theory, evidence theory firstly defines FD (a frame of discernment) Θ, which contains a set of mutually exclusive propositions. 2^{Θ} is a non-blank finite set that always denotes the power set of Θ, which means all possible various propositions. For example, if the frame of discernment Θ includes three mutually exclusive elementary propositions X_1, X_2 and X_3, the power set of Θ can be illustrated as follows

$$2^{\Theta} = \{\emptyset,\{X_1\},\{X_2\},\{X_3\},\{X_1,X_2\},\{X_1,X_3\},\{X_2,X_3\},\{X_1,X_2,X_3\}\} \quad (1)$$

In evidence theory, the probability is assigned not only to a single matter but also to any subset of possible propositions. m: $2^{\Theta} \rightarrow [0, 1]$, called as the BPAF (basic probability assignment function) of Θ, defines the elementary belief of each proposition, which should satisfy the following three theorems

Theorem 1: $m(A) \geq 0$ for any $A \in 2^{\Theta}$

Theorem 2: $m(\emptyset) = 0$

Theorem 3: $\sum_{A \subset \Theta} m(A) = 1$

where m(A) represents the corresponding BPAs of A. And every set A satisfying m(A) ≥ 0 be defined as a focal element.

It is hard to construct a precise PDF (probability density function) for proposition A because of the insufficient information or knowledge. Thus, it seems more reasonable to provide a confidence interval instead of a deterministic value to depict the total degree of belief in a proposition. In general, evidence theory uses the belief and plausibility to quantify the lower and upper bounds of an interval [Bel(A), Pl(A)], which is defined as

$$Bel(A) = \sum_{B \subseteq A} m(B) \quad (\forall A \subset \Theta) \tag{2}$$

$$Pl(A) = \sum_{A \cap B \neq \phi} m(B) \tag{3}$$

where Bel: $2^{\Theta} \rightarrow [0, 1]$ is called as belief which is obtained by adding the evidence of propositions in A. Meanwhile, Pl: $2^{\Theta} \rightarrow [0, 1]$ is the summation of BPAs that belong to the propositions of A totally or partially, which is defined as the Plausibility function of Θ.

1.2. Characteristic function with interval variables based on DS theory

Considering a general function with q-dimensional independent variables

$$Y = f(X) \quad X_i \in X,\ i = 1, 2, ..., q \tag{4}$$

Similar to the probability theory, the uncertain parameters are generally seen as relatively independent and the joint frame of discernment S is defined as

$$S = X_1 \times X_2 \times ... \times X_q = \{s_k = [x_1, x_2, ..., x_q],\ x_j \in X_j,\ j = 1, 2, ..., q\} \tag{5}$$

where s_k and x_j represent the focal element of joint FD and the focal element of the jth evidence variable, respectively. The joint BPAs can be expressed as

$$m_s(s_k) = \begin{Bmatrix} \prod_{j=1}^{q} m(x_j) \\ 0,\ otherwise \end{Bmatrix} \tag{6}$$

In probability theory, the mean value E(X) and the evidence variable X_i^I are relatively independent. However, the evidence variable X_i^I is an interval rather than a deterministic value. Thus, E(X) and X_i^I are related rather than independent. Based on the concepts mentioned above, considering the overestimation phenomenon in interval analysis, the characteristic function of evidence variables are provided below [31].

1.2.1. The relevant expectance E(X)

Through the analysis above, the relevant expectance $E(X_i)$ is expressed as

$$E(X_i) = \sum_{\substack{j=1 \\ j \neq i}}^{n} X_j^l / n \tag{7}$$

where n is the amount of evidence variables. X_j^l is the others except X_i^l.

1.2.2. The relevant variance $D'(X)$

Similar to the expectance E(*X*), the overestimation characteristics is also exited in the variance D(*X*) calculation. To eliminate the phenomenon above, expanding the E(*X*), the variance formula is defined as

$$\begin{aligned} D(X) = \sum_{i=1}^{n} (X_i^l - (X_1^l m(X_1^l) + X_2^l m(X_2^l) + ... + X_{i-1}^l m(X_{i-1}^l) + X_i^l m(X_i^l) \\ + X_{i+1}^l m(X_{i+1}^l) + ... + X_n^l m(X_n^l)))^2 m(X_i^l) \end{aligned} \tag{8}$$

where X_i^l is the *i*th evidence variable and $m(X_i^l)$ is the corresponding BPAs.

Obviously, D(*X*) changes with the change of X_{i} in the interval [Bel(*A*), Pl(*A*)]. Thus, the relevant variance $D'(X)$ can be defined as

$$D'(X) = \sum_{i=1}^{n} (\frac{n^2 - (1+\beta)n}{n(n-\beta)} X_i^l - (\sum_{\substack{j=1 \\ j \neq i}}^{n} X_j^l / n))^2 m(X_i^l) \tag{9}$$

where β is the interval correction coefficient and its range is from 0.01 to 0.30. The coefficient factor ∂ is introduced to the relevant variance, which is expressed as

$$\partial = \frac{n^2 - (1+\beta)n}{n(n-\beta)} \tag{10}$$

So, the relevant variance formula is rewritten as

$$D'(X) = \sum_{i=1}^{n} (\partial X_i^l - E(X_i))^2 m(X_i^l) \tag{11}$$

1.2.3. The relevant covariance $Cov'(X_1, X_2)$

Similarly, the co-relevant expectance $E'(X_i)$ is introduced for covariance Cov(X_1, X_2), which is defined as

$$E^{'}(X_i)=\sum_{\substack{j=1\\ j\neq i}}^{n} X_j^l\, m(X_j^l) \tag{12}$$

By introducing the coefficient factor δ to covariance, the relevant covariance $Cov^{'}(X_1, X_2)$ can be expressed as

$$Cov^{'}(X_1, X_2)=\sum_{i=1}^{n}\sum_{j=1}^{m}(\delta_1 X_{1i}^l - E^{'}(X_{1i}^l))(\delta_2 X_{2j}^l - E^{'}(X_{2j}^l))\, m(X_{1i}^l X_{2j}^l) \tag{13}$$

where $\delta_1=\frac{n}{n-\varepsilon_1}-m(X_{1i}^l)$, $\delta_2=\frac{m}{m-\varepsilon_2}-m(X_{2j}^l)$, ε_1 and ε_2 are the interval combined coefficients whose range is from 0.01 to 0.25.

2. FEM/RPIM for structural-acoustic coupling system

In this paper, the coupled FEM/RPIM method is proposed to solve the structural-acoustic field problem, in which the FEM/RPIM model is used to simulate the plate structure and the acoustic medium. Due to the c_0 continuity characteristic of fluid element, the Reissner-Mindlin plate is elected to the plate structure, in which the normals to the mid-plane of the plate remain straight during the deformation[32]. And the acoustic medium satisfies the linear constitutive equations which is assumed to be inviscid and incompressible. On the interface of the plate and the acoustic medium, only the acoustic medium exerts the normal loads on the plate and the normal displacement of the plate is just coupled with the acoustic medium[33].

2.1. FEM/RPIM model of the plate structure

In the frequency domain, without considering structural damping, the steady-state dynamic equation Galerkin weak form of the plate structure can be defined as

$$\begin{aligned}&\int_{\Omega}\delta\kappa^T D_b\kappa d\Omega+\int_{\Omega}\delta\gamma^T D_s\gamma d\Omega+\int_{\Omega}\delta\mu^T\rho t\omega^2\ddot{\mu}\,d\Omega\\&+\int_{\partial\Omega}\delta\mu^T t_s dS-\int_{\Omega}\delta\mu^T b_s d\Omega=0\end{aligned} \tag{14}$$

where $\boldsymbol{\mu}$ is the displacement, $\ddot{\mu}$ is the acceleration, $\boldsymbol{\rho}$ is the material density, $\boldsymbol{t}$ is the thickness of plate element, $\boldsymbol{t_s}$ is the surface loading plate structure and $\boldsymbol{b_s}$ is volume force, respectively.

γ and κ are the plate shear strain and bending strain, respectively, which can be expressed as:

$$\gamma = [\frac{\partial w}{\partial x} - \theta_x \quad \frac{\partial w}{\partial y} - \theta_y]^T \tag{15}$$

$$\kappa = [-\frac{\partial \theta_x}{\partial x} \quad -\frac{\partial \theta_y}{\partial y} \quad -(\frac{\partial \theta_x}{\partial y} = \frac{\partial \theta_y}{\partial x})]^T \tag{16}$$

$\boldsymbol{D_s}$ and $\boldsymbol{D_b}$ are the transverse shear stiffness constitutive matrix and the bending plate stiffness constitutive matrix, respectively, which are written as:

$$D_s = \frac{Et\nu}{2(1+\nu)}\begin{bmatrix} 1 & 0 \\ 0 & 1 \end{bmatrix} \tag{17}$$

$$D_b = \frac{Et^3}{12(1-\nu^2)}\begin{bmatrix} 1 & \nu & 0 \\ \nu & 1 & 0 \\ 0 & 0 & \frac{1-\nu}{2} \end{bmatrix} \tag{18}$$

where $\boldsymbol{E}$ is the Young's modulus, $\boldsymbol{\nu}$ is the Poisson's ratio and $\mathbf{v}$=5/6 is the shear correction factor, respectively.

From Eqs.(15-18), we can get that $\begin{bmatrix} \kappa \\ \nu \end{bmatrix} = \begin{bmatrix} B_b \\ B_s \end{bmatrix} \mu$, the steady-state dynamic equation of the plate structure is defined as

$$Ku - M\ddot{u} = F_f + F_b \tag{19}$$

where $\boldsymbol{K}$ denotes the plate stiffness matrix which is given as

$$\boldsymbol{K} = \boldsymbol{K}_b + \boldsymbol{K}_s = \int_\Omega (\boldsymbol{B}_b)^T \boldsymbol{D}_b \boldsymbol{B}_b d\Omega + \int_\Omega (\boldsymbol{B}_s)^T \boldsymbol{D}_s \boldsymbol{B}_s d\Omega \tag{20}$$

$\boldsymbol{K_b}$ denotes the the bending stiffness matrix, $\boldsymbol{K_s}$ denotes the shear stiffness matrix, $\boldsymbol{M}$ denotes the plate element mass matrix, $\boldsymbol{M}$ is defined as

$$M = \int_\Omega \rho Q^T diag[\frac{t^3}{12} \quad \frac{t^3}{12} \quad t] Q d\Omega \tag{21}$$

$\boldsymbol{F_f}$ and $\boldsymbol{F_b}$ are the surface load matrix and a volume force array, which are expressed as

$$F_f = \int_{\partial\Omega} Q^T t_s dS \tag{22}$$

$$F_b = \int_\Omega Q^T b_s d\Omega \tag{23}$$

2.2. FEM/RPIM model for the acoustic medium

In the engineering application, the fluid is generally regarded as compressible and inviscid which is seen to undergo small translational movement[34]. Considering an acoustic field problem with domain Ω_f and boundary Γ_b, the speed of sound ***c*** and the field acoustic pressure ***p*** are provided, the acoustic wave equation is defined as

$$\Delta p - \frac{1}{c^2}\frac{\partial^2 p}{\partial t^2} = 0, \text{ in } \Omega_f \tag{24}$$

where Δ is the Laplace operator, ***p*** is the field acoustic pressure, ***c*** and ***t*** are the speed of sound traveling in the fluid medium and its time, respectively.

The boundary condition of acoustic field is written as

$$\nabla p.n = 0 \quad , \quad \text{on} \quad F_b \tag{25}$$

where ***n*** denotes the boundary surface normal to the acoustic fluid domain.

On the interface between the plate structure and the acoustic medium, the momentum balance requires that

$$\nabla p.n = -\rho \ddot{u}_f \text{ on } \Omega_f \tag{26}$$

where ρ is the density of acoustic medium, $\ddot{u}_f$ is the normal acceleration component of acoustic fluid on the interface and Ω_f is the interface between the plate structure and acoustic fluid.

If the acoustic pressure ***p*** is regarded as a time harmonic variable, the Eq.(24) can be re-written as

$$\nabla^2 p + k^2 p = 0 \tag{27}$$

where $k = \omega / c$ represents the wavenumber, ω is the angular frequency, ***c*** denotes the sound speed.

The smoothed Galerkin weak form for acoustic problems can be expressed as

$$-\int_{\Omega}\nabla\Psi.\nabla\Psi P d\Omega+\frac{1}{c^2}\int_{\Omega}\Psi.\Psi P d\Omega-\rho\int_{\partial\Omega_{sf}}\Psi P.\ddot{u}_f\, d\Gamma-\int_{\Omega}\Psi.\Psi P.\frac{\partial q_f}{\partial t}d\Omega=0 \qquad (28)$$

where q_f is the additional load of unit volume and ψ expresses the shape function matrix of FE-RPIM.

For numerical computation, the acoustic wave equation should be discretized by using the Radial Point Interpolation method[35]. This leads to the discreted equation of node sound pressure $\boldsymbol{p}$ which is re-written as

$$p=\sum_{i=1}^{m}N_{f_i}p_i=N_f P \qquad (29)$$

where $\boldsymbol{p}$ is the vector of nodal pressure, $\boldsymbol{m}$ expresses the number of nodal variables per element, and $\boldsymbol{N}_f$ denotes the FE-RPIM shape function of fluid domain.

By substituting Eq.(29) into Eq.(28), the matrix form equation of acoustic domain can be obtained as

$$\boldsymbol{K}_f\boldsymbol{p}+\boldsymbol{M}_f\ddot{\boldsymbol{p}}=\boldsymbol{F}_f \qquad (30)$$

where $\boldsymbol{K}_f$ is the acoustic stiffness matrix and it can be expressed as

$$\boldsymbol{K}_f=\int_{\Omega}\boldsymbol{B}_f^{\mathrm{T}}\boldsymbol{B}_f\mathrm{d}\Omega \qquad (31)$$

$\boldsymbol{B}_f$ denotes the smoothed gradient matrix that is defined as

$$\boldsymbol{B}_f=\begin{bmatrix}\boldsymbol{\Psi}_{1,x} & \boldsymbol{\Psi}_{2,x} & \cdots & \boldsymbol{\Psi}_{M,x}\\ \boldsymbol{\Psi}_{1,y} & \boldsymbol{\Psi}_{2,y} & \cdots & \boldsymbol{\Psi}_{M,y}\\ \boldsymbol{\Psi}_{1,z} & \boldsymbol{\Psi}_{2,z} & \cdots & \boldsymbol{\Psi}_{M,z}\end{bmatrix} \qquad (32)$$

$\boldsymbol{M}_f$ is the acoustic mass matrix and it is written as

$$\boldsymbol{M}_f=\frac{1}{c^2}\int_{\Omega}\boldsymbol{\Psi}^{\mathrm{T}}\boldsymbol{\Psi}d\Omega \qquad (33)$$

$\boldsymbol{p}$ denotes the nodal pressure of the acoustic domain, which can be expressed as

$$\boldsymbol{p}=\{p_1,p_2,\cdots,p_n\}^{\mathrm{T}} \qquad (34)$$

$\boldsymbol{F}_s$ and $\boldsymbol{F}_f$ are the vectors of nodal acoustic forces that are given as

$$F_s = \rho \int_{\partial\Omega_{sf}} \Psi^T . \Psi d\Gamma \tag{35}$$

$$F_f = \int_{\Omega} \Psi^T \frac{\partial q_f}{\partial t} d\Omega \tag{36}$$

2.3. Coupled FEM/RPIM for structural-acoustic problem

Considering that the structural domain $\boldsymbol{\Omega}_s$ coupled with fluid domain $\boldsymbol{\Omega}_f$ on the interface $\boldsymbol{\Omega}_{sf}$, the boundary conditions of structural-acoustic coupling system are denoted by Γ_b, Γ_u and Γ_t which are illustrated in Fig.1. In this section, the coupled FEM/RPIM equation is proposed for structural-acoustic problem.

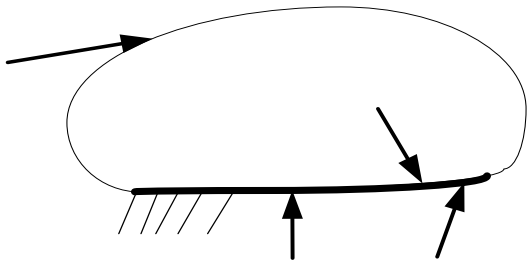

Figure 1. Schematic illustrating of the structural-acoustic system

The fluid particle and the structure move in the normal direction of the interface are written as

$$u_s \boldsymbol{n}_s = u_f \boldsymbol{n}_f \tag{37}$$

where $\boldsymbol{n}$ is the normal vector, $\boldsymbol{u_s}$ is the displacement of structure on the interface and $\boldsymbol{u_f}$ is the displacement of fluid contacting the structure.

On the interface, based on the continuity and equilibrium conditions, we obtain that $\boldsymbol{n}=\boldsymbol{n_f}=-\boldsymbol{n_s}$[36]. The fluid force loading on the structure $\boldsymbol{F_s}$ can be expressed as

$$\begin{aligned} \boldsymbol{F}_s &= \int_{\Omega_{sf}} \boldsymbol{N}_s^T \boldsymbol{n}_s \sigma_s d\Gamma_f = \int_{\Omega_{sf}} \boldsymbol{N}_s^T n_f p d\Gamma_f \\ &= \left(\int_{\Omega_{sf}} \boldsymbol{N}_s^T \boldsymbol{n}_f \boldsymbol{N}_f d\Gamma_f \right) \boldsymbol{p} \end{aligned} \tag{38}$$

The structural force loading on the fluid $\boldsymbol{F_f}$ is also expressed as

$$
\begin{aligned}
F_f &= -\rho \int_{\Omega_{sf}} N_f^T \ddot{u}_f \, d\Gamma = -\rho \int_{\Omega_{sf}} N_f^T \ddot{u}_s \, d\Gamma \\
&= -\rho \left(\int_{\Omega_{sf}} N_f^T n_f N_s d\Gamma \right) \ddot{u}_s
\end{aligned} \tag{39}
$$

The spatial coupling matrix $\boldsymbol{H}$ can be defined as

$$
\boldsymbol{H} = \int_{\Omega_{sf}} \boldsymbol{N}_s \boldsymbol{n}_f \boldsymbol{N}_f dS \tag{40}
$$

By substituting the Eq.(40) into Eq.(38) and Eq.(39), the equations are rewritten as

$$
\boldsymbol{F}_s = \boldsymbol{H}\boldsymbol{p} \qquad [redacted] = -\rho \boldsymbol{H}^T \ddot{\boldsymbol{u}}_s \tag{41}
$$

Thus, the governing equation for coupled structure-acoustic system is expressed as

$$
\begin{bmatrix} \boldsymbol{M} & 0 \\ \rho \boldsymbol{H}^T & \boldsymbol{M}_f \end{bmatrix} \begin{Bmatrix} \ddot{\boldsymbol{u}}_s \\ \ddot{\boldsymbol{p}} \end{Bmatrix} + \begin{bmatrix} \boldsymbol{K} & -\boldsymbol{H} \\ 0 & \boldsymbol{K}_f \end{bmatrix} \begin{Bmatrix} \boldsymbol{u}_s \\ \boldsymbol{p} \end{Bmatrix} = \begin{Bmatrix} \boldsymbol{F}_s \\ \boldsymbol{F}_f \end{Bmatrix} \tag{42}
$$

Assuming that the displacement and pressure are all time-harmonic[37], Eq.(42) can be rewritten as

$$
\begin{bmatrix} \boldsymbol{K} - \omega^2 \boldsymbol{M} & -\boldsymbol{H} \\ \rho \omega^2 \boldsymbol{H}^T & \boldsymbol{K}_f - \omega^2 \boldsymbol{M}_f \end{bmatrix} \begin{Bmatrix} \boldsymbol{u}_s \\ \boldsymbol{p} \end{Bmatrix} = \begin{Bmatrix} \boldsymbol{F}_s \\ \boldsymbol{F}_f \end{Bmatrix} \tag{43}
$$

To simplify the process of analyzing the FE/RPI equation of the structural-acoustic system[38,39], we rewrite Eq. (43) into the following form

$$
ZU = F \tag{44}
$$

where $\boldsymbol{Z}$ is the structural-acoustic dynamic stiffness matrix, $\boldsymbol{U}$ is the response vector and $\boldsymbol{F}$ is the external excitation vector which can be expressed as

$$
Z = \begin{bmatrix} K - \omega^2 M & -H \\ \rho \omega^2 H^T & K_f - \omega^2 M_f \end{bmatrix}, \quad U = [u_s \;\; p]^T, \quad F = [F_s \;\; F_f] \tag{45}
$$

3. DS-FE/RPIM for epistemic uncertainty structural-acoustic problem

Discretizing the structural-acoustic coupling system, the discretization form of the structural-acoustic dynamic stiffness matrix $\boldsymbol{Z}$ and the external excitation vector $\boldsymbol{F}$ can be rewritten as

$$
Z = \begin{bmatrix} \sum_{i=1}^{N} K_i - \omega^2 \sum_{i=1}^{N} M_i & -\sum_{i=1}^{N} H_{fi} \\ \rho \omega^2 [\sum_{i=1}^{N} H_{fi}]^T & \sum_{i=1}^{NA} K_{fi} - \omega^2 \sum_{i=1}^{NA} M_{fi} \end{bmatrix} \tag{46}
$$

$$F = \{\sum_{i=1}^{N} F_{si} \ \sum_{i=1}^{NA} F_{fi}\} \tag{47}$$

where ***N*** denotes the number of plate elements and ***NA*** denotes the number of acoustic field elements, respectively.

According to D-S evidence theory, the FPD of the dynamic stiffness matrix and the external excitation vector in evidence focal element are expressed as

$$\frac{\partial Z(X_{ik}^{m})}{\partial X_{ik}} = \begin{bmatrix} \sum_{i=1}^{N} \frac{\partial K_i}{\partial X_{ik}} - \omega^2 \sum_{i=1}^{N} \frac{\partial M_i}{\partial X_{ik}} & -\sum_{i=1}^{N} \frac{\partial H_{fi}}{\partial X_{ik}} \\ \rho\omega^2 [\sum_{i=1}^{N} \frac{\partial H_{fi}}{\partial X_{ik}}]^T & \sum_{i=1}^{NA} \frac{\partial K_{fi}}{\partial X_{ik}} - \omega^2 \sum_{i=1}^{NA} \frac{\partial M_{fi}}{\partial X_{ik}} \end{bmatrix} \tag{48}$$

$$F = \{\sum_{i=1}^{N} \frac{\partial F_{si}}{\partial X_{ik}} \ \sum_{i=1}^{NA} \frac{\partial F_{fi}}{\partial X_{ik}}\}^T \tag{49}$$

where X_{ik}^{m} is the interval variable which denotes the ***k***th focal element of the ***i***th evidence variable.

Combined with the interval perturbation theory, ignoring the higher order perturbation[40], the approximate formula of node pressure response is defined as

$$p_{ik}^{m} = (Z_{ik}^{m})^{-1} F_{ik}^{m} \tag{50}$$

$$\begin{aligned} \Delta p_{ik}^{I} &= (Z_{ik}^{m})^{-1} (\Delta F_{ik}^{I} - \Delta Z_{ik}^{I} p_{ik}^{m}) \\ &= (Z_{ik}^{m})^{-1} \left\{ \Delta X_{ik} \left(\frac{\partial F(X_{ik}^{m})}{\partial X_{ik}} - \frac{\partial Z(X_{ik}^{m})}{\partial X_{ik}} p_{ik}^{m} \right) \Delta e^{I} \right\} \end{aligned} \tag{51}$$

where p_{ik}^{m} is the node pressure and $\boldsymbol{\Delta e^{I}}$=[-1, 1].

According to Eq.(51), the estimated value of Δp_{ik}^{I} interval radius is expressed as

$$\Delta p_{ik} = \left| (Z_{ik}^{m})^{-1} \Delta X_{ik} \frac{\partial F(X_{ik}^{m})}{\partial X_{ik}} \right| + \left| (Z_{ik}^{m})^{-1} \Delta X_{ik} \frac{\partial Z(X_{ik}^{m})}{\partial X_{ik}} p_{ik}^{m} \right| \tag{52}$$

Based on the value range of evidence vector, under the effects of the evidence variable $\boldsymbol{X_{ik}}$, the upper and lower bounds of the node pressure response value p_{ik}^{m} can be write as

$$p_{ik}^{U} = p_{ik}^{m} + \Delta p_{ik} \tag{53}$$

$$p_{ik}^{L} = p_{ik}^{m} - \Delta p_{ik} \tag{54}$$

By substituting Eq.(53) and Eq.(54) to Eq.(7), the expectance interval of the steady-state sound pressure response can be expressed as

$$E(p)^{U} = \sum_{i=1}^{I} \sum_{\substack{k=1 \\ k \neq j}}^{n} P_{ik}^{U} / n \tag{55}$$

$$E(p)^{L} = \sum_{i=1}^{I} \sum_{\substack{k=1 \\ k \neq j}}^{n} P_{ik}^{L} / n \tag{56}$$

where $\boldsymbol{I}$ is the number of the evidence variables and $\boldsymbol{n}$ denotes the number of focal elements, respectively.

By substituting Eqs.(53-56) to Eq.(9), the deviation interval of the sound pressure response is expressed as

$$D(p)^{U} = \sum_{i=1}^{I} (\sum_{j=1}^{n} (\frac{n^2 - (1+\beta)n}{n(n-\beta)} p_{ij}^{U} - E(p)^{U})^2 m_{ij}) \tag{57}$$

$$D(p)^{L} = \sum_{i=1}^{I} (\sum_{j=1}^{n} (\frac{n^2 - (1+\beta)n}{n(n-\beta)} p_{ij}^{L} - E(p)^{L})^2 m_{ij}) \tag{58}$$

4. Numerical example

In this section, a 3D structural-acoustic problem is provided to verify the approach mentioned above. A square flexible plate model coupled with the acoustic field of dimensions 500×500×500mm is depicted in Fig.2. The plate structure is discretized by 144 four-node quadrilateral elements and the acoustic field is discretized by 1152 eight-node hexahedron elements. The acoustic field is surrounded by five rigid walls and a flexible plate. The plate is excited by a unit normal harmonic point force at the middle point and the boundary conditions for it are: $\boldsymbol{w}$ = 0, and $\boldsymbol{\theta_x}$ and $\boldsymbol{\theta_y}$ are free at the edges.

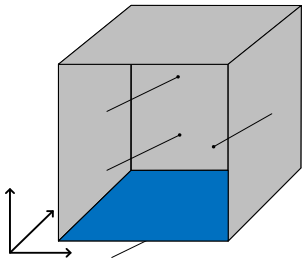

Figure 2. A cubic structural-acoustic coupling model

The density $\boldsymbol{\rho_s}$ and the Poisson's ratio $\boldsymbol{v}$ of the plate are 2.5×10^3 kg/m^3 and 0.37, respectively. The sound speed of the air in the acoustic field $\boldsymbol{c}$ is 346m/s. The Young's modulus and the thickness of the plate, the density of the air in the acoustic field are considered to be the independent uncertain parameters which are treated as evidence variables. To compare with the probability method, assumed that the evidence variables are the truncated normal distribution: $\boldsymbol{\mu(E)}$=21×10^4Mpa, $\boldsymbol{\sigma(E)}$=0.84×10^4 Mpa, $\boldsymbol{\mu(\rho_f)}$=1.30 kg/m^3, $\boldsymbol{\sigma(\rho_f)}$=0.03kg/m^3 and $\boldsymbol{\mu(t)}$=1.25mm, $\boldsymbol{\sigma(t)}$=0.05mm. The BPA of uncertain parameters with 4, 8 and 16 focal elements are given in Table 1. Simulations of the cubic structural-acoustic coupling model are carried out by MATLAB R2009a on a 3.30 GHz Xeon(R) CPU E3 1230 v3.

Table 1. The BPA for uncertain parameters with 4, 8 and 16 focal elements

focal elements	E (10^4 MPa)		ρ_f (kg/m^3)		t (mm)	
	focal element	BPA	focal element	BPA	focal element	BPA
4	[18.50, 19.75]	6.69	[1.21, 1.26]	6.55	[1.10, 1.18]	6.55
	[19.75, 21.00]	43.16	[1.26, 1.30]	43.30	[1.18, 1.25]	43.30
	[21.00, 22.25]	43.16	[1.30, 1.34]	43.30	[1.25, 1.33]	43.30
	[22.25, 23.50]	6.69	[1.34, 1.39]	6.55	[1.33, 1.40]	6.55
8	[18.50, 19.13]	1.13	[1.21, 1.23]	1.08	[1.10, 1.14]	1.09
	[19.13, 19.75]	5.56	[1.23, 1.26]	5.45	[1.14, 1.18]	5.46
	[19.75, 20.38]	16.00	[1.26, 1.28]	15.98	[1.18, 1.21]	15.97
	[20.38, 21.00]	27.16	[1.28, 1.30]	27.34	[1.21, 1.25]	27.33
	[21.00, 21.63]	27.16	[1.30, 1.32]	27.34	[1.25, 1.29]	27.33
	[21.63, 22.25]	16.00	[1.32, 1.35]	15.98	[1.29, 1.33]	15.97
	[22.25, 22.88]	5.56	[1.35, 1.37]	5.45	[1.33, 1.36]	5.46
	[22.88, 23.50]	1.13	[1.37, 1.39]	1.08	[1.36, 1.40]	1.09
16	[18.50, 18.81]	0.31	[1.21, 1.22]	0.30	[1.10, 1.12]	0.29
	[18.81, 19.13]	0.82	[1.22, 1.23]	0.79	[1.12, 1.14]	0.78
	[19.13, 19.44]	1.86	[1.23, 1.24]	1.82	[1.14, 1.16]	1.82
	[19.44, 19.75]	3.69	[1.24, 1.26]	3.64	[1.16, 1.18]	3.64
	[19.75, 20.06]	6.38	[1.26, 1.27]	6.35	[1.18, 1.19]	6.35

[20.06, 20.38]	9.62	[1.27, 1.28]	9.63	[1.19, 1.21]	9.63
[20.38, 20.69]	12.65	[1.28, 1.29]	12.71	[1.21, 1.23]	12.72
[20.69, 21.00]	14.52	[1.29, 1.30]	14.61	[1.23, 1.25]	14.62
[21.00, 21.31]	14.52	[1.30, 1.31]	14.61	[1.25, 1.27]	14.62
[21.31, 21.63]	12.65	[1.31, 1.32]	12.71	[1.27, 1.29]	12.72
[21.63, 21.94]	9.62	[1.32, 1.33]	9.63	[1.29, 1.31]	9.63
[21.94, 22.25]	6.38	[1.33, 1.35]	6.35	[1.31, 1.33]	6.35
[22.25, 22.56]	3.69	[1.35, 1.36]	3.64	[1.33, 1.34]	3.64
[22.56, 22.88]	1.86	[1.36, 1.37]	1.82	[1.34, 1.36]	1.82
[22.88, 23.19]	0.82	[1.37, 1.38]	0.79	[1.36, 1.38]	0.78
[23.19, 23.50]	0.31	[1.38, 1.39]	0.30	[1.38, 1.40]	0.29

The relevant expectance and standard deviation of the sound pressure response at the points with the distances of 50mm, 100mm, 150mm, 200mm, 250mm, 300mm, 350mm, 400mm, 450mm and 500mm are calculated. In Fig. 3, the results of frequency 100 Hz are depicted. The lower and upper bounds of the relevant expectance and standard deviation of the sound pressure response at the Point 1 with the distance of 400mm in the frequency range of 20 to 200 Hz are plotted in Fig. 4. The results obtained by the Monte Carlo method with 100000 samples are used as the reference. From Fig. 3 and Fig. 4, when the uncertain parameters are treated as evidence variables, the relevant expectance and standard deviation of the sound pressure response are intervals. Besides, the lower and upper bounds of the relevant expectance and standard deviation contain the reference. With the number of focal elements increasing, the width of the expectance and standard deviation will be decreased. Because of each evidence variable follows the truncated normal distribution in which the BPA of focal element is the cumulative probability distribution in the corresponding interval. With the amount of information increasing, the evidence uncertainty could be reducible. Thus, the analysis results will more approach to the probability computational results with more BPAs in a certain interval range. In the numerical example, the precision and effectiveness of the proposed approach for structural-acoustic fields with epistemic uncertainty is validated by comparing the analysis results with evidence variables to the probability computational results.

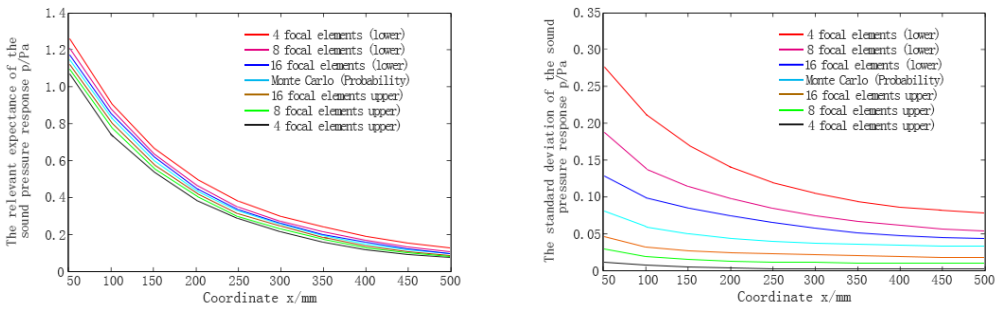

Figure 3. Bounds of the relevant expectance and standard deviation of the sound pressure response with 4, 8 and 16 focal elements (100Hz)

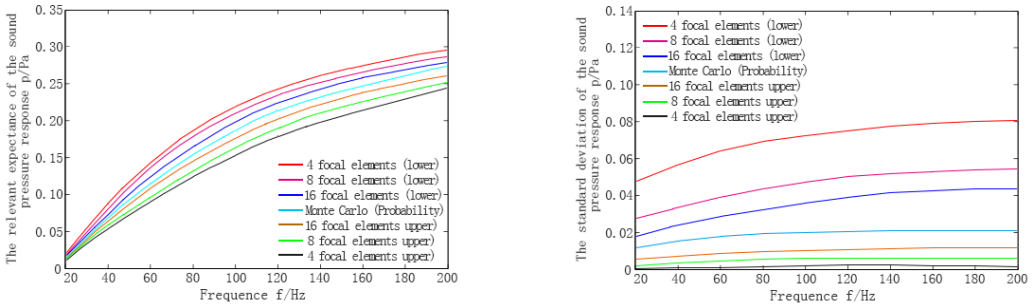

Figure 4. Bounds of the relevant expectance and standard deviation of the sound pressure response at the Point 1 under 4, 8 and 16 focal elements (20 - 200 Hz)

Assuming that $\boldsymbol{x}$ is an evidence variable and $\boldsymbol{X}$ denotes the sound pressure response, the belief Bel ($\boldsymbol{X} \leq \boldsymbol{x}$) and the plausibility Pl ($\boldsymbol{X} \leq \boldsymbol{x}$) of the sound pressure response at the Point 2 for the frequency 100 Hz are depicted in Fig. 5. The probability density function (PDF) of probability computational results obtained by the Monte Carlo method with 100000 samples are also regarded as the reference. From Fig.5, the PDFs are surrounded by the Bels and the Pls. Furthermore, with the number of focal elements increasing, the width between Bel and Pl will be decreased which further indicates the precision and effectiveness of the proposed method.

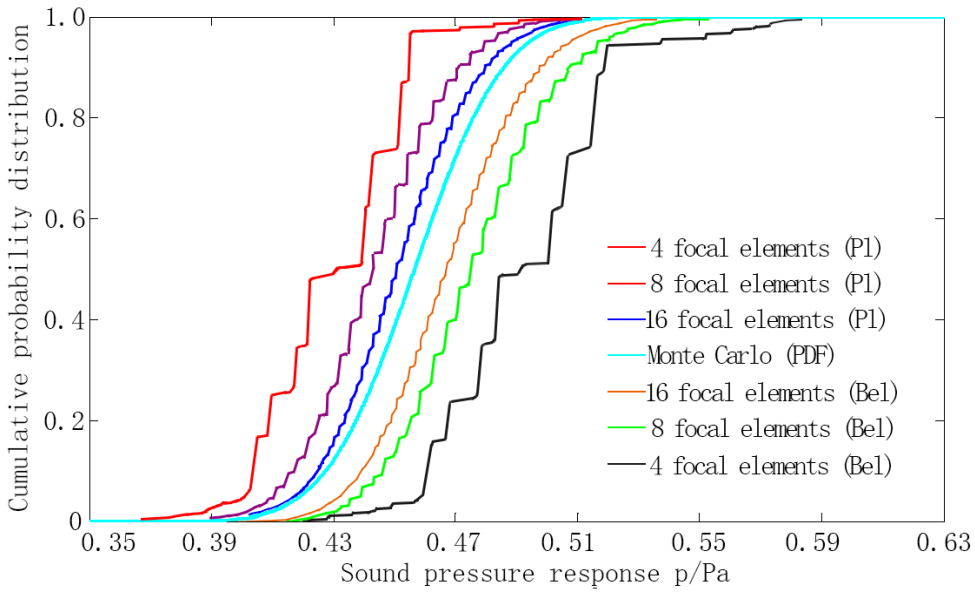

Figure 5. Cumulative probability distribution of the sound pressure response at the Point 2 (100Hz)

Conclusions

In this paper, an evidence-theory-based approach is proposed for structural-acoustic problem with epistemic uncertainty. The evidence theory is used to handle the epistemic uncertainty in which there is no enough information or sufficient knowledge to construct the precise probability distribution for uncertain parameters. The numerical example of a plate structure-acoustic coupling system is investigated. The conclusions are as follows:

(1) The overestimation phenomenon, which derives from the correlation between parameters, is widely existent in the analysis of complex systems. The proposed method is suggested to overcome the characteristic of overestimation. The results of the numerical example shows that the proposed approach is much more efficient than the original method as the focal elements increases. Therefore, we can control the form, size and quantity of focal element to improve the analytical accuracy in practical applications.

(2) The relevant expectance, standard deviation and probability density distribution of sound pressure response are intervals not deterministic values. As the amount of information and knowledge increasing, the epistemic uncertainty could be eliminated. In other words, the bandwidths of the relevant expectance, standard deviation and probability density distribution of sound pressure response will be narrower which means the analysis results will more approach to the probability computational results.

It should be noted that this paper is focused on the epistemic uncertainty. In practical engineering problems, epistemic uncertainty and aleatory uncertainty may exist simultaneously. Thus, in further research, on the one hand, the hybrid evidence variables and random variables involved in structural-acoustic field will be investigated. On the other hand, the proposal method could be widely applied in engineering fields, such as dynamic thermal field analysis, thermal-coupling field analysis, heat-pressure field analysis and so on.

Acknowledgments

The paper is supported by the Independent Research Project of State Key Laboratory of Advanced Design and Manufacturing for Vehicle Body in Hunan University (Grant No. 71375004 and Grant No. 51375002) and the Hunan Provincial Innovation Foundation for Postgraduate (Grant No. CX2014B147). The authors would also like to thank reviewers for their valuable suggestions.

REFERENCE

[1] Du, J. B., Olhoff, N. (2010) Topological design of vibrating structures with respect to optimum sound pressure characteristics in a surrounding acoustic medium, Struct. Multi. Optim. 42 (1), 43–54.

[2] He, Z. C., Liu, G., R., Zhong, Z. H., Zhang, G. Y., Cheng, A. G. (2011) A coupled ES-FEM/BEM method for fluid–structure interaction problems, Eng. Anal. Bound Elem. 35, 140–7.

[3] Chen, N., Yu, D., Xia, B. (2015) Evidence-theory-based analysis for the prediction of exterior acoustic field with epistemic uncertainties, Eng. Anal. Bound Elem. 50, 402-411.

[4] Stefanou, G. (2009) The stochastic finite element method: past, present and future, Comput. Method Appl. M. 198 (9–12), 1031–1051.

[5] Hoffman, F. O., Hammonds, J.S. (1994) Propagation of uncertainty in risk assessment: the need to distinguish between uncertainty due to lack of knowledge and uncertainty due to variability, Risk Anal. 14 (5), 707–12.

[6] Zhan, K., Luo, Y. (2009) Non-probabilistic reliability-based topology optimization of

geometrically nonlinear structures using convex models, Comput. Methods Appl. Mech. Eng. 198 (41), 3228–38.

[7] Adhikari, S. (2011) Doubly spectral stochastic finite-element method for linear structural dynamics, J. Aerospace Eng. 24 (3), 264–276.

[8] Feng, Y. T., Li, C. F., Owen, D. R. J. (2010) A directed Monte Carlo solution of linear stochastic algebraic system of equations, Finite Elem. Anal. Des. 46 (6), 462–473.

[9] Hua, X. G., Ni, Y. Q., Chen, Z. Q., Ko, J. M. (2007) An improved perturbation method for stochastic finite element model updating, Int. J. Numer. Meth. Eng. 73 (13), 1845–1864.

[10] Oberkampf, W. L., Helton, J. C. Investigation of evidence theory for engineering applications, AIAA2002-1569, Non-Deterministic Approaches Forum, Denver, CO; 2002.

[11] Jiang, C., Zhang, Z., Han, X., Liu, J. (2013) A novel evidence-theory-based reliability analysis method for structures with epistemic uncertainty, Comput. Struct. 129, 1–12.

[12] Bai, Y. C., Jiang, C., Han, X., Hu, D. A. (2013) Evidence-theory-Based structural static and dynamic response analysis under epistemic uncertainties, Finite Elem. Anal. Des. 68, 52-62.

[13] Bae, H. R., Grandhi, R. V., Canfield, R. A. (2006) An approximation approach for uncertainty quantification using evidence theory, Reliab. Eng. Syst. Saf. 86, 215–225.

[14] Bae, H. R., Grandhi, R. V., Canfield, R. A. (2004) Epistemic uncertainty quantification techniques including evidence theory for large-scale structures, Comput. Struct. 82, 1101–1112.

[15] Helton, J. C., Johnson, J. D., Oberkampf, W. L., Sallaberry, C. J. (2006) Sensitivity analysis in conjunction with evidence theory representations of epistemic uncertainty, Reliab. Eng. Syst. Saf. 91, 1414-1434.

[16] Haim, Y. Ben, Elishakoff, I. Convex Models of Uncertainty in Applied Mechanics, Elsevier Science Publishers, Amsterdam, 1990.

[17] Qiu, Z. P., Xia, Y. Y., Yang, J. L. (2007) The static displacement and the stress analysis of structures with bounded uncertainties using the vertex solution theorem, Comput. Methods Appl. Mech. Eng. 196 (49–52), 4965–84.

[18] Helton, J. C., Johnson, J. D., Oberkampf, W. L. (2004) An exploration of alternative approaches to the representation of uncertainty in model predictions, Reliab. Eng. Syst. Saf. 85, 39-71.

[19] Rao, S. S., Berke, L. (1997) Analysis of Uncertain Structural Systems Using Interval Analysis, AIAA 35 (4), 727-735.

[20] Massa, F., Tison, T., Lallemand, B. (2006) A fuzzy procedure for the static design of imprecise structures, Comput. Methods Appl. Mech. Eng. 195 (9–12), 925–941.

[21] Gersem, H. De, Moens, D., Desmet, W., Vandepitte, D. (2007) Interval and fuzzy dynamic analysis of finite element models with superelements, Comput. Struct. 85 (5–6), 304–319.

[22] Balu, A.S., Rao, B.N. (2012) High dimensional model representation based formulations for fuzzy finite element analysis of structures, Finite Elem. Anal. Des. 50, 217–230.

[23] Hanss, M., Turrin, S. (2010) A fuzzy-based approach to comprehensive modeling and analysis of systems with epistemic uncertainties, Struct. Saf. 32 (6), 433–441.

[24] Bae, H. R., Grandhi, R. V., Canfield, R. A. (2006) An approximation approach for uncertainty quantification using evidence theory, Reliab. Eng. Syst. Saf. 86, 215-225.

[25] Bae, H. R., Grandhi, R. V., Canfield, R. A. (2004) Epistemic uncertainty quantification techniques including evidence theory for large-scale structures, Comput. Struct. 82, 1101-1112.

[26] Soundappan, P., Nikolaidis, E., Haftka, R. T., Grandhi, R., Canfield, R. (2004) Comparison of evidence theory and Bayesian theory for uncertainty modeling. Reliab. Eng. Syst. Saf. 85 (1), 295–311.

[27] Xia, B., Yu, D., Liu, J. (2013) Interval and subinterval perturbation methods for a structural-acoustic system with interval parameters, J. Fluid. Struct. 38, 146-163.

[28] Heaney, K. D., Cox, H. (2006) A tactical approach to environmental uncertainty and sensitivity, IEEE J. Oceanic Eng. 31, 356–367.

[29] Xia, B., Yu, D., Liu, J. (2013) Hybrid uncertain analysis for structural–acoustic problem with random and interval parameters, J. Sound Vib. 332, 2701-2720.

[30] Dehghan, M., Hashemi, B. (2006) Iterative solution of fuzzy linear systems, Appl. Math. Comput. 175, 645–74.

[31] Elishakoff, I., Thakkar, K. (2014) Overcoming Overestimation Characteristic to Classical Interval Analysis, AIAA Journal 52 (9), 2093-2097.

[32] Xia, B., Yu, D. (2014) An interval random perturbation method for structural-acoustic system with hybrid uncertain parameters, Int. J. Numer. Meth. Engng. 97, 181-206.

[33] Xia, B., Yu, D., Liu, J. (2013) Probabilistic Interval Perturbation Methods for Hybrid Uncertain Acoustic Field Prediction, J. Vib. Acoust. 135, 1-12.

[34] Everstine, G. C., Henderson, F. M. (1990) Coupled finite element/boundary element approach for fluid structure interaction, J. Acoust. Soc. Am. 87, 1938-1947.

[35] Wenterodt, C., Estorff, O. Von (2009) Dispersion analysis of the meshfree radial point interpolation method for the Helmholtz equation, Int. J. Numer. Meth. Engng. 77, 1670-1689.

[36] Li, K., Huang, Q. B., Wang, J. L., Lin, L. G. (2011) An improved localized radial basis function meshless method for computational aeroacoustics, Eng. Anal. Bound Elem. 35, 47-55.

[37] Zhang, Z., Jiang, C., Han, X., Hu, Dean, Yu, S. (2014) A response surface approach for structural reliability analysis using evidence theory, Adv. Eng. Softw. 69, 37-45.

[38] He, Z. C., Liu, G. R., Zhong, Z. H., Cui, X. Y., Zhang, G. Y., Cheng, A. G. (2010) A coupled edge-/face-based smoothed finite element method for structural-acoustic problems, Appl. Acoust. 71, 955-964.

[39] Wang, C., Qiu, Z., Wang, X., Wu, D. (2014) Interval finite element analysis and reliability-based optimization of coupled structural-acoustic system with uncertain parameters, Finite Elem. Anal. Des. 91, 108-114.

[40] Xia, B., Yu, D., Han, X., Jiang, C. (2014) Unified response probability distribution analysis of two hybrid uncertain acoustic fields, Comput. Methods Appl. Mech. Engrg. 276, 20-34.